Cite as: S. Majumder, S. A. Khaparde, A. P. Agalgaonkar, S. V. Kulkarni, A. K. Srivastava, and S. Perera, "Chance-Constrained Pre-Contingency Joint Self-Scheduling of Energy and Reserve in a VPP," IEEE Trans. Power Syst., Jan. 2023 [Accepted].

Chance-Constrained Pre-Contingency Joint Self-Scheduling of Energy and Reserve in a VPP

Subir Majumder, *Member, IEEE,* Shrikrishna A. Khaparde, *Senior Member, IEEE,* Ashish P. Agalgaonkar, *Senior Member, IEEE,* S. V. Kulkarni, *Fellow, IEEE,* Anurag K. Srivastava, *Fellow, IEEE,* Sarath Perera, *Senior Member, IEEE*

***Abstract*—With the increasing penetration of primarily inertia-less distributed energy resources, allowable delay in the fast frequency reserve provision to ensure marginal stability condition can become comparable with the requisite dead-time for fast-switching in a radial power distribution system (PDS) connected to the transmission system. Consequently, the prevailing short-duration load-generation imbalance might propagate as system-wide frequency excursion in the future power system, which traditionally has not been observed. Furthermore, during the fast-switching, some of the fast-acting reserve (FAR) providing local generators remain inaccessible to the bulk power system (BPS). This work has answered the questions of requisite reserve requirements to cater to such events through efficient energy and FAR provision joint-scheduling. Stochasticity of fast-switching, with temporary faults as a use-case, requires modeling of load-generation imbalance and local resource unavailability, vis-á-vis FAR requirement problem, as a chance-constraint. Due to the limited visibility at the BPS level, PDS operators must ensure sufficient FAR availability for a given confidence level of the chance-constraint. Individual chance-constraints are used to ensure mathematical simplicity. Here, the PDS is operated as a virtual power plant (VPP), where the operator can procure resources locally or from the wholesale market with the aim of profit maximization before the contingency occurs. Results show that FAR requirements can influence the local energy schedule and raise energy costs. Furthermore, the confidence level of the chance-constraint can impact overall profitability, and FAR should be scheduled carefully. Comparative analysis with a modified benchmark IEEE 33-node radial test system and a 98-node test system shows the superior performance of the proposed approach. The impact of the limited available FAR is also demonstrated.**

***Index Terms*—Chance-Constrained Optimization, Day-Ahead Market, Fast-Switching, Joint-Scheduling, Low-Inertia Power System, Reserve Allocation, Virtual Power Plants (VPP)**

NOMENCLATURE

$\gamma_{q,y,t}$	Demand response (DR) level y, of the load connected at bus q, during interval t, ($\in \{0,1\}$).
η_{ch}, η_{dch}	Aggregated charging and discharging efficiency of the battery storage devices (BSDs), in *pu*.
π_t^{DR}	Retail price of electricity for the customers during interval t, in MU/kW.
$\pi_t^{E/RF/RS}$	Energy /fast-acting reserve (FAR) /primary frequency reserve (PFR) price in the electricity market during interval t, in MU/kW.
τ	Duration for which FAR needs to be dispatched from BSDs, in h.
κ	The confidence level of the chance-constraint.
$\Xi_t^+,\ \beta_{\xi,t}^+$	Parameters of the conditional value-at-risk problem to cater to load insufficiency.
$\Xi_t^-,\ \beta_{\xi,t}^-$	Parameters of the conditional value-at-risk problem to cater to generation insufficiency.
$\mathfrak{C}^{B/DG}$	Total daily operational cost of BSDs/diesel generators (DGs) in the energy market, in MU.
$\mathfrak{C}^{DiG/DR}$	Total daily operational cost of renewable energy generators (REGs)/controllable loads, in MU.
$\mathfrak{C}^{WEM}$	Cost of power purchase from the day-ahead wholesale market, in MU.
k_t	Hour equivalent of scheduling intervals, in h^{-1}.
$\mathfrak{L}_y, \mathscr{P}_y^{DR}$	Change in load demand and price of electricity at DR level y, in %.
$\mathfrak{R}_{q,t}^{DG}$	Ramp rate of DGs located at bus q during interval t, in kWh^{-1}.
$S_{0,t}, S_{q,t}^{DG}$	PFR procured from the market and allocated from the DG located at bus q, during interval t, in kW.
$P_{l,t}^{flow}$	Active line flow during interval t, of line, l.
$Q_{l,t}^{flow}$	Reactive power line flow during interval t, of line, l.
$\mathcal{S}_l$	Flow limit of line, l.
$\mathrm{A}_{\xi,q}$	Parameter identifying whether node q remains connected during the event ξ.
$\mathrm{D}_q^{B/DiG}$	Unit cost of power production from the BSDs/REGs located at bus q, in MU/kW.
$\mathcal{J}_{q,t}, \mathbb{B}_{q,t}$	Commitment status of the DG and total energy stored within the BSD located at bus q respectively, at the end of the interval t, in KWh.
RUD_t	Both up and down PFR requirements during interval t, in kW.

Subir Majumder was with the Department of Energy Science and Engineering at Indian Institute of Technology Bombay, Mumbai 400076, India, the School of Electrical, Computer and Telecommunications Engineering at University of Wollongong, NSW 2522, Australia. He is now working with the Lane Department of Computer Science and Electrical Engineering at West Virginia University, WV 26506, USA (e-mail: subirmajumder@iitb.ac.in).

S. A. Khaparde was and S. V. Kulkarni is with the Department of Electrical Engineering at Indian Institute of Technology Bombay, India.

Ashish P. Agalgaonkar is and Sarath Perera was with the School of Electrical, Computer and Telecommunications Engineering at University of Wollongong, NSW 2522, Australia.

Anurag K. Srivastava is with the Lane Department of Computer Science and Electrical Engineering at West Virginia University, WV 26506, USA.

This work was partially supported by the IPTA and UPA Scholarship from UOW, MHRD of GoI and from the DOE UI-ASSIST grant.

$\mathbb{B}_q^{ini}$	Initial stored charge within BSDs located at bus q, in kWh.
$\mathbb{B}_q^{min/max}$	Minimum/maximum stored charge within BSDs located at bus q, in kWh.
$C_{q,l}$	Bus-branch connectivity matrix among line, l, and node, q.
$E_{q,t}^{B}$	The FAR allocation schedule from BSDs at bus q for interval t, in kW.
$E_{q,t}^{DiG/DR}$	The FAR allocation schedule from REGs/controllable loads at bus q for interval t, in kW.
$E_{q,t}^{tot}, P_{q,t}^{tot}$	An effective total local FAR and energy generation schedule at bus q for the interval t, in kW.
$E_{0,t}^{BR}, P_{0,t}^{G}$	Total FAR and energy purchased from the energy market by the virtual power plant operator, for the interval t, in kW.
pf_q	Peak load power factor of the load connected at bus q, during interval t.
$P_{q,t}^{L}, Q_{q,t}^{DR}$	Forecast of the load and reactive power demand of DR customer, respectively, connected at bus q, during interval t.
$P_{q,t}^{B,+/-}$	Power injected or extracted into the BSD at the grid end of bus q, during interval t, in kW.
$P_{q,t}^{DG/DiG}$	Power to be provided from DGs/REGs located at bus q, during interval t, in kW.
$P_{q,t}^{DR}$	Power consumed by the DR loads located at bus q, during interval t, in kW.
$P_{q}^{DG,max}$	Power generation upper limit of the DGs, in kW.
$P_{q}^{DG,min}$	Power generation lower limit of the DGs, in kW.
$P_{q,t}^{DiG,MPP}$	Forecasted maximum power generation of the REGs located at bus q, during interval t, in kW.
$P_{q,t}^{L,max}$	Upper convenience limit of the demand responding load located at bus q during interval t, in kW.
$P_{q,t}^{L,min}$	Lower convenience limit of the demand responding load located at bus q during interval t, in kW.
r_l, x_l	Resistance and reactance of branch l, in Ω.
$V_{q,t}, V_{0,t}$	Node voltage of bus q, and reference voltage during interval t, in kV.
$z_{q,t}$	Charging or discharging status of BSDs, located at bus q, during interval t ($\in \{0,1\}$).

I. Introduction

A. Background & Literature Review

LIMITED capacity prevents direct participation of individual distributed energy resources (DERs) into the wholesale electricity market (WEM). Virtual power plants (VPPs) [1] provide an alternative in this regard through an aggregation approach. Although there is a significant amount of literature on VPPs [2], [3], their practical implementations through pilot projects have started only recently. In this regard, facilitated by the recently passed Federal Energy Regulatory Commission (FERC) order 2222 [4] in the United States, DER operators can participate in the wholesale electricity market through an aggregator. One such pilot project example would be in the Electric Reliability Council of Texas (ERCOT) [5], where qualified DERs are able to participate in the wholesale day-ahead energy and non-spinning reserve market. Here, ERCOT identifies one/multiple logical resource nodes for telemetry and metering, where telemetry consists of an aggregated representation of all the resources within VPP premises. VPP demonstration project is also notable in Southern Australia (SA) power networks [6] where the net solar exporters are remunerated through a premium feed-in tariff (FIT) mechanism. Although increased telemetry with smart grid deployment increases DER visibility to the VPP, these resources have limited visibility to bulk power system operators. Secondly, contrary to the FIT mechanism, Time-Of-Use (TOU) tariff captures the time value of electricity facilitating regulation of electricity demand [7].

Given the limited visibility, it is the responsibility of the utility company/retailers, acting as a VPP operator, to ensure that local disturbances do not propagate into the bulk power system (BPS) or the associated impact remains invisible to the BPS operator. Furthermore, the consensus is that DERs would soon replace conventional generators as the primary form of generation. However, these DERs primarily include inverter-based resources (IBR) that contribute little to no inertia to the BPS; and consequently, it is expected that the aggregated system inertia, vis-á-vis inertial reserve of the BPS, would continue to decline. Owing to persisting residual inertia within the grid [8], [9], the system's inertia would remain nonzero. Therefore, the operation of the grid with increasing penetration of inverter-based DERs can be highly challenging.

As stated in [10], faster-acting frequency responsive resources, such as IBRs, will be important in the reduced synchronous resources paradigm. Accordingly, this work utilizes a term called fast-acting reserve (FAR) to symbolize the use of such resources for inertial support. However, unlike synchronous resources, these IBRs do not inherently respond to the system frequency, and one needs to rely on frequency measurements for the inertial support from these resources. Local frequency measurements can be noisy, and hence, the use of multiple data sources across various locations for frequency control is also suggested in the literature [11]. Requisite collection of multiple data streams and requisite processing for the decision-making makes this frequency estimation (based on which IBRs are expected to respond) inherently delayed. Additionally, the response time of IBRs (DERs in general), although very small, can quickly add up, leading to delayed FAR provision [11]. However, if inertia-less generators' response is quick enough, delayed-droop control as a part of FAR provision can still limit the post-contingency frequency excursion [12], and local DERs can participate in such an endeavor. Furthermore, a recent report prepared for the FERC [13] suggests the participation of DERs, including renewable energy generator (REGs)-based IBRs, in the frequency response. While both of the pilot projects discussed earlier facilitate the provision of reserve into the bulk grid, there are concerns about how variable renewable resources would contribute towards system inertia.

The electricity distribution networks, where DERs are typically connected, may often require fast-switching. Here, the fast-switching requirement due to faults in the power distribution system (PDS) is considered as a use-case. Since a majority of the faults in the PDS are temporary [14], we will restrict our focus to temporary faults. During the post-fault system operation, the first objective is to isolate and contain the fault, which is carried out by the coordinated operation of fuses, reclosers, and sectionalizers [15]. Fuse-saving recloser operation is usually advocated to improve the system average interruption frequency index (SAIFI) of the network [16]. Consequently, the faulted section will remain isolated from the rest of the PDS, vis-á-vis the BPS, for a small but finite time with due consideration of coordination and reclosing delay or dead time [17]. Alongside, some of the FAR-providing DERs will also remain isolated. Therefore, reliable FAR provision from these DERs can be very challenging. Furthermore, the disconnection of a segment within the PDS during the dead-time would also create a temporary load-generation imbalance within the BPS. Again, once the recloser closes and the normal operating condition is reinstated, DERs need to be appropriately synchronized before they are brought back online [18]. *Although load-generation imbalance is not a significant concern for traditional power system operation, reducing system inertia would make this problem very difficult to overcome.*

As shown in Fig. 1, therefore, from VPPs point of view, it will be crucial to ensure that the local load-generation imbalance remains contained by ensuring sufficient FAR provision. VPPs may procure FAR from local resources or could be purchased from the electricity market so that the BPS operator is ignorant of these local events. Since the occurrence of temporary faults is uncertain, FAR must be procured well in advance (e.g., say, in the day-ahead market) to be able to be dispatched in real-time. One of the possible ways in which VPPs can bid into the day-ahead WEM would be to provide self-schedules since the market operators typically do not readjust self-scheduling resources [19]. VPP may self-schedule its resources to provide energy and frequency reserve in the WEM. Notably, the FAR requirement to mitigate the load-generation imbalance is a function of the operating schedule of local resources, which is also not known apriori. In this work, we consider that (i) the loads and generators are paid at a retail rate (such as TOU tariffs), (ii) VPPs typically have the cost characteristics of local resources, and (iii) VPPs are capable of calculating local DER forecasts, to be able to derive the day-ahead self-schedule. Since the variability in the renewable generation and load demands are relatively slower, one would require primary-frequency reserve (PFR) alongside much-needed energy demand, making our problem an energy, PFR, and FAR self-scheduling problem.

Simultaneous allocation of energy and reserve based on the associated marginal costs leading to an efficient provision is well known. In the context of the use of risk constraints for VPPs, among the recently published literature, [20] discusses bilevel decision-making with minimal financial risk with financial transmission rights, [21] considers robust optimization with multiple endo- and exogenous uncertainties, [22] considers multi-horizon information-gap decision theory, and [23] considers coordinated aggregator and VPP models. The economic FAR allocation methodology through a joint-scheduling strategy to mitigate the effect of reduced inertia with fast-switching, considering temporary faults as a use-case, in a PDS has been identified as a research gap.

B. Problem Statement

In one of the earlier works by authors [12], it has been shown that allowable latency to ensure marginal stability condition of the power system in the delayed frequency control of the power system declines with system inertia. If the allowable delay is comparably smaller than the dead-time for the recloser operation, the local load-generation imbalance due to fast-switching requirements with temporary faults will propagate as frequency excursion into the BPS. Since the BPS operator is invisible to events within VPP premises, a VPP operator is expected to procure sufficient FAR, either from local resources or from the WEM, to cater to these events. These reserves are required to be procured sufficiently ahead, but the reserve requirements are subject to forecast uncertainty and event uncertainty. Additionally, following temporary faults, there are two challenges in the operation of the future power system with significant penetration of IBRs: (i) local load-generation imbalance can propagate in the form of frequency excursion into BPS, (ii) some of the local FAR providing DERs may be disengaged from the BPS. Stochasticity of temporary faults demands using the risk-constrained model for FAR provision. Since reserve requirements are a function of local schedules and worst-case optimal power flow (OPF) solution, (i) may not exist or (ii) cost-prohibitive, we need to carry out chance-constrained joint-self-schedule to identify the bidding strategy for the VPP into the day-ahead WEM.

Fast-switching driven identification of reserve requirements, especially in the future low-inertia power system context, has never been discussed before to the best of the knowledge of the authors (see [24] in this regard) and is the major contribution of this work. It is imminent that this phenomenon can significantly influence the operation of a PDS with a significantly higher fault rate. In this work, the following research questions are answered: (i) probabilistically, how much FAR to procure? (ii) where to procure it from? (iii) when is it most needed? and (iv) is there any correlation between fault-rate and FAR requirements? FAR requirements due to other events requiring fast-switching can be suitably incorporated but not described here for brevity. The scope of this work is limited to VPP self-scheduling in the day-ahead market, which also satisfies the early FAR procurement criterion. Notably, the dispatch can significantly change in real-time due to various possible forecast errors. However, the impact of associated uncertainties in FAR procurement is not considered here.

C. Contributions

The contributions of this work are threefold:

(a) Probability of the fast-switching operation has been derived in this work considering temporary faults as an

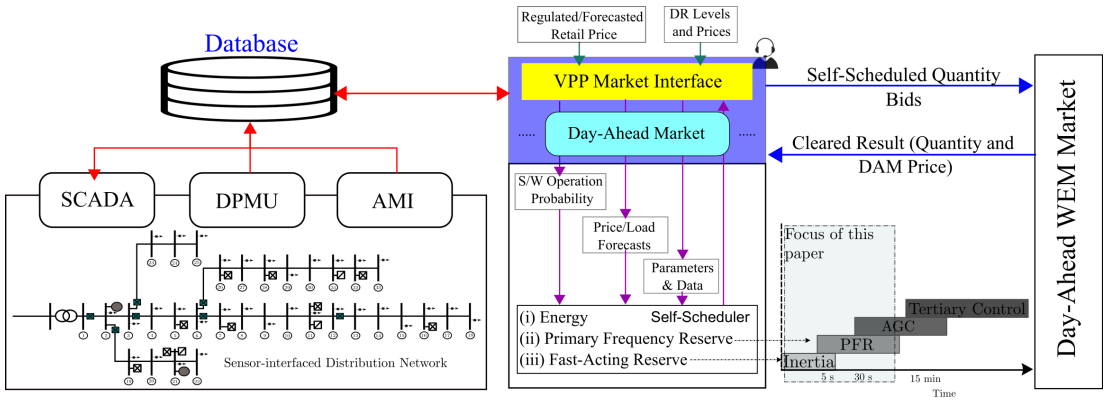

Figure 1: Overview of the proposed DA joint self-scheduling problem.

example. These probabilities are calculated considering the fault rate of the distribution lines following non-homogeneous Poisson distribution to capture the likelihood of the occurrence of faults with seasonal variability. The condition under which the said probabilistic definitions become unusable has been described, and it is notable that robust optimization methodology can be utilized in such cases.

(b) Conditional value at risk (CVaR) measure has been utilized to ensure FAR sufficiency catering to load-generation imbalance for the VPP during fast-switching up to a specific confidence level. FAR requirements are a function of the local resource schedule and the location of faults within the network. Given the value at risk (VaR) measure implies chance-constraints, and, VaR is always less than that of CVaR, the proposed formulation guarantees the satisfaction of the chance-constraint. The CVaR approximation of the loss function is also shown to be convex, making the chance-constrained reserve and energy provisioning problem as a mixed-integer linear programming (MILP) problem.

(c) The impact of temporary faults on FAR requirements is studied considering a modified IEEE 33-bus radial PDS from the VPPs perspective. Availability of FAR from the battery storage devices (BSDs), controllable loads, and REGs is considered. Energy and reserve requirements from local resources and the WEM in the day-ahead temporal horizon are analyzed. The impact of the confidence level of the chance-constrained problem on the overall profitability of the VPP is also discussed, which has facilitated the performance analysis of chance-constraints. The solutions are also contrasted against worst-case solutions. Comparative dynamic performance of the system with limited FAR has been discussed. The scalability of the proposed formulation has been demonstrated using a moderately sized 98-node radial test system.

D. Paper Organization

The remainder of the paper is organized as follows. Calculation of probabilities for recloser operation, FAR requirements, the chance-constrained optimization problem, and calculation of reserve requirements from various sources have been described in Section II. VPP price taker joint-scheduling model has been described in Section III. The proposed methodology has been illustrated using a modified IEEE 33-bus and a 98-bus radial PDS and is presented in Section IV. Section V includes the concluding remarks.

II. FAR Requirements of Future VPPs

A. Rate of Operation of Reclosers

Figure 2 shows a typical radial PDS, wherein, supposedly, two reclosers J_1 and J_2 are in place. Fault-rate of a section of the PDS connected between bus q and bus r is given by ℓ_{qr}. The fault-rate in the case of the overhead distribution lines is a function of several parameters, and a detailed discussion in this regard can be found in [14] and [25]. It is to be noted that the fault rates in case of overhead distribution lines[1] can vary throughout the year and even for each and every scheduling interval. Two fault scenarios, namely $\mathcal{Z}_1$ and $\mathcal{Z}_2$, as depicted in Fig. 2, are identified.

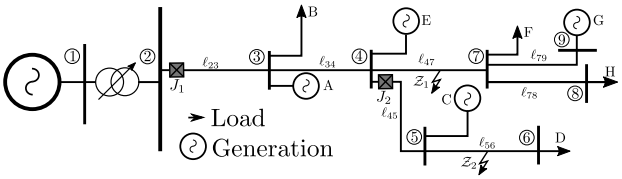

Figure 2: A schematic diagram of a VPP.

Given a faulted condition, only a particular set of reclosers would operate. For example, given scenario $\mathcal{Z}_1$ occurs, both reclosers J_1 and J_2 would operate to isolate the fault expecting that the fault clears within the reclosing delay. Furthermore, if the fault occurs on either of lines 2-3, 7-8, and 7-9, the set of reclosers J_1 and J_2 would still operate. For the faulted condition $\mathcal{Z}_2$, the only recloser J_2 would operate. Similarly, J_2 operates if the fault also occurs on lines 4-5. Furthermore, from the PDS point of view, in the considered scenarios, three different event types can be assumed, such as (i) operation of

[1]Since faults in the underground cables majorly lead to permanent faults and given temporary faults is the considered use-case associated fault rates are ignored in the probability calculation.

J_1 and J_2, (ii) operation of J_2 alone, and (iii) no operation of recloser(s).

A generalized definition of the set of event types representing reclosers' operation in a radial PDS is given below:

Definition 1. *Following the occurrence of a fault within a radial PDS, at least one of the local reclosers would operate for fuse-saving operation. Suppose, for isolating a temporary fault, the event type ξ has occurred, and in this process, an immediately upstream recloser,* uu*, operates. Suppose* vv *is the set of all the reclosers connected at downstream of* uu*. Let* ww *be the set of reclosers connected downstream of any of the reclosers from set* vv*, such that* ww $\subset$ vv *(note the properness). If O_{uu} is the set of all lines connected downstream of a recloser,* uu*, then the rate of occurrence of event type, ξ, will be λ_ξ, and can be given by,*

$$\lambda_\xi = \sum_{\forall \mathrm{y} \in O_{\mathrm{uu}}} \ell_{\mathrm{y}} - \sum_{\forall \mathrm{z} \in O_{\mathrm{vv}\setminus\mathrm{ww}}} \ell_{\mathrm{z}} \tag{1}$$

where, y *and* z *are indices identifying distribution lines and ℓ_{y} represents fault rate of line* y*.* □

In case of a change in PDS topology (say the network becomes weakly meshed), the event types in Definition 1 would also need to be modified. Here, a set of possible unique recloser combinations for the successful isolation of faults with minimal impact on the loads can be defined as event types.

If a fault occurs outside of PDS premises (beyond the transmission and distribution system interface boundary), certain relays would still operate to prevent feeding the fault. The probability of occurrence of events within the BPS (external to the PDS) is ignored here. However, the occurrence of these external events needs to be taken care of by the WEM operators to ensure reserve sufficiency within the entire power system. The protection system within PDS is typically taken care of by coordinated operation of relays, reclosers, sectionalizers, and various circuit-breakers. Locations of protection devices other than reclosers have been ignored in this work, being one of the faster devices to respond and dedicated to minimizing the impacts of temporary faults.

B. Probabilities of Event Types

Typically, the considered interval of interest in the identification of the fault statistics is large enough, and the rate of occurrence of faults within a given interval is shown to follow the Poisson distribution[2] [25], [14]. However, looking at the number of daily occurrences of faults, these events appear in clusters associated with weather events [26]. This is one of the reasons behind the seasonally varying fault-rate model depicted in [27], which is in stark contrast with the homogeneous Poisson process model discussed earlier. Alternatively, a non-homogeneous Poisson point process model could be utilized. Under this case, the Poisson parameter, defined on a real line, is time-dependent [28]. The occurrence of faults relies on different environmental parameters, and fault rates can vary seasonally or even multiple times in a day, which can be forecasted for the Poisson parameter. Although the probability of occurrence of faults in the power system daily is demonstrated to follow power law distribution, such a relationship may vary from system to system. For example, in [29], modeling clustered events as a Poisson process, and power-law distribution underestimates and overestimates the event probabilities. Although, as shown in [26], the cluster model better captures these events. However, clusters cannot be identified before the events have actually passed. Therefore, from the day-ahead scheduling point of view, the analysis is limited by an interval-to-interval basis.

Event occurrence probability, according to power law distribution, will be greater than the Poisson process if the expected number of events is approximately equal to the Poisson parameter. Both power law distribution and Poisson distribution have a long tail if the Poisson parameter is less than one (see tail section of the Poisson distribution in Fig. 2.11 of [29]). Ignoring the extremely rare events and probabilities associated with these long tails (which may not be accurate during extreme weather events resulting in multiple contingencies), the event space could be simplified quite significantly while also facilitating the identification of an analytical expression of the event occurrence probabilities.

It is well known that implicit probability distribution for chance-constraints is not always known, and therefore these problems are difficult to solve [30]. In the absence of implicit probability distributions, typically, one uses Monte-Carlo sampling techniques to identify random discrete scenarios [31]. Since these scenarios are randomly generated, one needs to perform out-of-sample tests to find the robustness of the identified solution. However, considering the fault events as a non-homogeneous point process gives us mathematical simplicity by allowing us to model switching events as individual chance-constraints with interval-wise implicit event occurrence probability. Therefore, it has been considered that the event type, ξ, as discussed earlier, would follow a non-homogeneous Poisson probability distribution.

The probability that $\mathfrak{c}$ number of events of event type ξ occur within an interval of duration k_t, $\mathbb{P}_{\xi,\mathfrak{c},t}$, is:

$$\mathbb{P}_{\xi,\mathfrak{c},t} = e^{-\lambda_{\xi,t}k_t} \frac{(\lambda_{\xi,t}k_t)^{\mathfrak{c}}}{\mathfrak{c}!} \tag{2}$$

Here, $\lambda_{\xi,t}$ is the rate of occurrence of event type ξ during interval t (time-dependent rate parameter). The probability that event type, ξ does not occur, $\mathbb{P}_{\xi,0,t}$, is given by,

$$\mathbb{P}_{\xi,0,t} = 1 - \sum_{\mathfrak{c}=1}^{\infty} e^{-\lambda_{\xi,t}k_t} \frac{(\lambda_{\xi,t}k_t)^{\mathfrak{c}}}{\mathfrak{c}!} = e^{-\lambda_{\xi,t}k_t} \tag{3}$$

The probability that at least one event of type ξ occurs, $\mathbb{P}_{\xi,\geq 1,t}$, is given by,

$$\mathbb{P}_{\xi,\geq 1,t} = 1 - e^{-\lambda_{\xi,t}k_t} \tag{4}$$

The time-varying rate of occurrence of event type, ξ, during interval t, which is given by $\lambda_{\xi,t}$, can be very small. It is considered that the longevity of the concerned interval, k_t, is given by a typical scheduling interval (such as hourly [32] or 15 minutes [33] or 5 minutes [34]). This leads $\lambda_{\xi,t}k_t$ to become tiny (less than one as discussed above and close to zero). Consequently, an approximated calculation of the probabilities of each event type is sought (ignoring the tails as discussed above). Within a given interval of k_t, the probability

[2]Poisson process definition cannot be used when the randomness of events cannot be guaranteed.

of occurrence of more than one event of a given type is minuscule (but not zero). As a result, the occurrence of an event of a given event type, ξ, can be generalized to be 'event ξ'. Associated probability (using (4)) can be given by $(1-e^{-\lambda_{\xi,t}k_t})$. The probability of occurrence of different events can be obtained considering the independent nature of the events[3]. Given u and v are two different non-null events, the probability that none of the events occurs, $\mathbb{P}_{0,t}$, will be,

$$\mathbb{P}_{0,t} = \prod_{\forall \xi} e^{-\lambda_{\xi,t}k_t} = e^{-\sum_{\forall \xi}\lambda_{\xi,t}k_t} \approx 1 - \sum_{\forall \xi}\lambda_{\xi,t}k_t \quad (5)$$

The probability, $\mathbb{P}_{\mathrm{u},t}$, that only event u occurs:

$$\mathbb{P}_{\mathrm{u},t} = e^{-\sum_{\forall \xi,\ \mathrm{u}\neq\xi}\lambda_{\xi,t}k_t}\left(1-e^{-\lambda_{\mathrm{u},t}k_t}\right) \approx \left(1-\sum_{\forall \xi,\ \mathrm{u}\neq\xi}\lambda_{\xi,t}k_t\right)\lambda_{\mathrm{u},t}k_t \approx \lambda_{\mathrm{u},t}k_t \quad (6)$$

The probability, $\mathbb{P}_{\mathrm{u,v},t}$, that events u and v concurrently occur within the same interval:

$$\mathbb{P}_{\mathrm{u,v},t} = e^{-\sum_{\forall \xi,\ \mathrm{u}\neq\mathrm{v},\xi}\lambda_{\xi,t}k_t}\left(1-e^{-\lambda_{\mathrm{u},t}k_t}\right)\left(1-e^{-\lambda_{\mathrm{v},t}k_t}\right) \approx 0 \quad (7)$$

Remark 1. *The probability of occurrence of more than one event type within a given interval will be approximately zero if* $1 > \sum_{\forall \xi}\lambda_{\xi,t}k_t \to 0$. *Therefore, the event probabilities comprising of: (i) occurrence of none of the events with probability,* $\mathbb{P}_{\varnothing,t}$, *and (ii) occurrence of events,* ξ, *with probabilities,* $\mathbb{P}_{\xi(\neq\varnothing),t}$, *encapsulate the entire probability space,* $\mathscr{N}$. □

Remark 2. *The calculated probabilities might not hold during extreme weather events, wherein* $\lambda_{\xi,t}k_t$ *could be* > 1. *Also, the probability of simultaneous occurrence of events, although negligible, is never zero. Consequently, event types as described in Remark 1 may not be entirely valid. However, for the problem at hand, those events can be safely ignored.* □

The applicability of the proposed risk-constrained methodology is limited due to the prior knowledge of fault probability distribution. Robust optimization can be used otherwise.

C. Power Imbalance and FAR Requirement during an Event

Following materialization of the event, ξ, suppose, $\{\mathrm{A}_{\xi,q} : \forall q\}$ be a vector representing the set of buses in the PDS being disconnected from the BPS during the recloser dead-time. The load-generation imbalance seen at the BPS, $P^{Imb}_{\xi,t}$, assuming load and generation remaining unchanged during an interval t for an event ξ, can be calculated as,

$$P^{Imb}_{\xi,t} = \sum_{\forall q\in\mathcal{I}}\left(P^{L}_{q,t} - P^{G}_{q,t}\right)\mathrm{A}_{\xi,q} \quad (8)$$

Here, $P^{L}_{q,t}$, $P^{G}_{q,t}$, are total load and generation respectively at bus q ($\in\mathcal{I}$), during interval t. Also, $\mathcal{I}$ is the set of all nodes within the PDS premises. If, $E^{tot}_{q,t}$ is the local FAR provision at bus q, the total reserve available during the interval t, $E^{Imb}_{\xi,t}$, corresponding to occurrence of event ξ, can be calculated as,

$$E^{Imb}_{\xi,t} = \sum_{\forall q\in\mathcal{I}} E^{tot}_{q,t}\left(1-\mathrm{A}_{\xi,q}\right) + E^{BR}_{0,t} \quad (9)$$

[3]From the day-ahead point of view the causality of events is not known, and therefore, the occurrence of temporary faults at different branches of the PDS remains fairly independent.

It is to be noted that the FAR traded from the WEM, independent of the occurrence of local events, $E^{BR}_{0,t}$, is always accessible.

D. Generation and Load Reserve Sufficiency as Risk Constraints

For an effective reserve allocation when the system-wide load is more than generation, the difference between the available reserve, $E^{Imb}_{\xi,t}$, and the requirement, $P^{Imb}_{\xi,t}$ has to remain positive to satisfy the worst-case scenario. However, solutions to worst-case optimization problems may not exist or may even be difficult to solve [30]. Alternatively, chance-constraints could be used where the reserve requirements are required to satisfy within a certain confidence level, κ, where the imbalance is probabilistically positive within this confidence level. However, as discussed earlier, chance-constrained problems require implicit probability distribution of random events, which is occasionally known. In those cases, one often utilizes Monte-Carlo sampling to estimate the probability distribution of those random events, with the possible consequence of modeling error in the long tails. Another possible consequence of modeling a chance-constrained problem is non-convexity within the constraint. A detailed literature review on convexification methodologies of chance-constraints is given in [30]. Nevertheless, as the confidence level tends to 1 if the tails in the probability distribution are appropriately modeled, the chance-constrained OPF solution converges towards the worst-case solution. We will compare both of these solutions.

The equivalence of chance-constraints and VaR is shown in [31] and elaborated in the Appendix. However, given the discreteness of the event types, VaR is a discontinuous and non-convex function. CVaR, also known as mean excess loss, guarantees convexity if the loss function is convex. Also, there are two ways of handling the chance-constraints: (i) joint chance-constraints, where all the constraints are required to be simultaneously satisfied up to a certain confidence level, or (ii) individual chance-constraints, with each of the constraints individually required to be satisfied up to the confidence level. The use of individual and joint chance-constraints for solving OPF problems are reported in [35] and [36], respectively. Owing to the consideration of the non-homogeneous Poisson process model for fast-switching considered in this work, interval-wise event occurrences are independent of each other. Therefore, one can limit its applicability to individual chance-constraints. Furthermore, individual chance-constraints provide numerical simplicity compared to joint chance-constraints involving multiple intervals.

Sufficient reserve availability for each of the operating intervals can be represented by the following chance-constraint,

$$\mathbb{P}\left(\sum_{\forall\xi\in\mathscr{N}}\left(P^{Imb}_{\xi,t} - E^{Imb}_{\xi,t}\right)\mathbb{1}_{\mathscr{N}}(\xi) \le 0\right) \ge \kappa; \quad \forall t \quad (10)$$

It is to be noted that $\left(P^{Imb}_{\xi,t} - E^{Imb}_{\xi,t}\right) \le 0$ symbolizes lost reserve availability corresponding to the event ξ within the probability space $\mathscr{N}$ (i.e., the requirement is less than

the availability). Also, $\mathbb{1}_{\mathcal{N}}(\xi)$ is an indicator function, which symbolizes, if the random event, ξ, is true, then $\mathbb{1}_{\mathcal{N}}(\xi) = 1$. In the current context, because the probability space is discrete, $\text{CVaR}_{\kappa}\left(\sum_{\forall\xi\in\mathcal{N}}\left(P^{Imb}_{\xi,t} - E^{Imb}_{\xi,t}\right)\mathbb{1}_{\mathcal{N}}(\xi)\right)$ during interval t can be computed as follows:

$$\text{CVaR}_{\kappa}\left(\sum_{\forall\xi\in\mathcal{N}}\left(P^{Imb}_{\xi,t} - E^{Imb}_{\xi,t}\right)\mathbb{1}_{\mathcal{N}}(\xi)\right) = \Xi^{+}_{t} + \frac{1}{1-\kappa}\sum_{\forall\xi\in\mathcal{N}}\mathbb{P}_{\xi,t}[P^{Imb}_{\xi,t} - E^{Imb}_{\xi,t} - \Xi^{+}_{t}]^{+} \quad (11)$$

Here, $[(\cdot)]^{+}$ represents the function $\max(0,(\cdot))$. To ensure reserve sufficiency, $\text{CVaR}_{\kappa}\left(\sum_{\forall\xi\in\mathcal{N}}\left(P^{Imb}_{\xi,t} - E^{Imb}_{\xi,t}\right)\mathbb{1}_{\mathcal{N}}(\xi)\right)$ needs to be negative for all the intervals. Therefore,

$$\Xi^{+}_{t} + \frac{1}{1-\kappa}\sum_{\forall\xi\in\mathcal{N}}\mathbb{P}_{\xi,t}\beta^{+}_{\xi,t} \leq 0; \quad \forall t \quad (12)$$

$$\left(P^{Imb}_{\xi,t} - E^{Imb}_{\xi,t}\right) - \Xi^{+}_{t} - \beta^{+}_{\xi,t} \leq 0; \quad \beta^{+}_{\xi,t} \geq 0; \quad \forall\xi, t \quad (13)$$

Ξ^{+}_{t} and $\beta^{+}_{\xi,t}$ are parameters of the CVaR problem. In this problem, CVaR is a conservative approximation of the chance-constraints[4]. It is imminent that the CVaR is efficiently computable and monotonic [37]. The proof of convexity with CVaR approximation is given in the following corollary:

Corollary 1. *The CVaR approximation of the chance-constraint is convex.*

Proof. Without loss of generality, the current chance-constrained problem can be stated in the following form:

$$\mathbb{P}\left(\sum_{\forall\xi}\mathrm{x}_{\xi}\mathbb{1}(\xi) \leq 0\right) \geq \kappa$$

The CVaR approximate as identified in [31] would be:

$$\Xi + \frac{1}{1-\kappa}\sum_{\forall\xi}\mathbb{P}_{\xi}\beta_{\xi} \leq 0$$

$$\mathrm{x}_{\xi} - \Xi - \beta_{\xi} \leq 0; \quad \beta_{\xi} \geq 0; \quad \forall\xi$$

This is the special case of sublinearity in Corollary 11 in [38]. Considering x_{ξ} as a parameter, it is imminent that CVaR constraints result in a system of inequalities. Given the half-spaces determined by the inequalities are convex, a system of inequalities would lead to the intersection of half-spaces which is also convex. □

In (10), the reserve insufficiency has been obtained from (8), wherein power imbalance is resulting from the load insufficiency point of view (i.e., $P^{Imb}_{\xi,t}$ is positive when the net disconnected load is more than the net generation disconnected, and the additional reserve is required to meet the excess generation). Additionally, depending on the spatiotemporal occurrence of temporary faults, the system may have an excess load. An additional chance-constraint needs to be incorporated to account for generation insufficiency, which is given as follows:

$$\mathbb{P}\left(\sum_{\forall\xi\in\mathcal{N}}\left(-P^{Imb}_{\xi,t} - E^{Imb}_{\xi,t}\right)\mathbb{1}_{\mathcal{N}}(\xi) \leq 0\right) \geq \kappa; \quad \forall t \quad (14)$$

Suitable additional constraints need to be considered to incorporate this additional CVaR condition. Associated constraints are discussed in detail in the Appendix.

Remark 3. *A more generalized chance-constraint where one can procure different amounts of up and down FAR from the WEM is possible.* □

Remark 4. *Some of the nodes within the PDS can form temporary microgrids (this will be true, especially for permanent faults) and hence, remain energized. However, the said problem is being looked at from the BPS point of view (disturbances in the PDS should not propagate to the BPS), and hence, the formation of microgrids is beyond the scope of this work. If required, these chance-constraints can also be adopted for the microgrids.* □

III. Price-Taker Joint-Self-Scheduling Strategy

A. Assumptions for Joint-Scheduling

As discussed earlier, the main objective of the proposed research is to analyze FAR requirements to cater to the fast-switching requirements with temporary faults as a use case. Both PFR and FAR are required at a finer time scale, but they must be procured much earlier, given the event's uncertainty. Therefore, the problem is analyzed from the day-ahead point of view, where the VPP participates in the WEM to procure energy, PFR, and FAR, as shown in Fig. 1. While the customers are expected to respond to the retail rate (in real-time), given the access to diesel generators (DGs), DERs cost function, and the customers' response characteristics (common knowledge to VPPs and consumers), the VPP identifies its self-schedule to participate in the day-ahead WEM, and provide associated set-point advisory to the associated participant. The end user (customers) provide their demand forecast, and due to the slow-moving nature, it is envisaged that automated hierarchical controllers will take care of the controlling part in FAR participation [39] (receiving set-point advisory and provide demand estimate to VPPs). The VPP is expected to forecast DER generation, which would also help in obtaining the self-schedule.

Notably, as we move closer to the real-time operation, any deviation in the forecast would result in further load generation imbalance, which would change FAR requirements. The change in FAR requirements in real-time is beyond the scope of this work. However, loads and REG variabilities are not entirely ignored in this work since, given coupled nature of the joint-scheduling problem, energy, PFR, and FAR requirements may constrain each other. It is considered that PFR requirements are a certain fraction of the load demand for simplicity. Provision of a short burst of power at a high ramp rate would be a major requirement for FAR providers, and

[4]As shown in the Appendix, VaR naturally follows from chance-constraints but is a discontinuous and non-convex function in the current context. However, CVaR being a convex relaxation of VaR, it does not guarantee that chance-constraints will be satisfied. Although VaR calculation is extremely complex, especially with discrete variables, typically, VaR $\leq$ CVaR [31]. Therefore, $\text{VaR}_{\kappa}\left(\sum_{\forall\xi\in\mathcal{N}}\left(P^{Imb}_{\xi,t} - E^{Imb}_{\xi,t}\right)\mathbb{1}_{\mathcal{N}}(\xi)\right) \leq \text{CVaR}_{\kappa}\left(\sum_{\forall\xi\in\mathcal{N}}\left(P^{Imb}_{\xi,t} - E^{Imb}_{\xi,t}\right)\mathbb{1}_{\mathcal{N}}(\xi)\right) \leq 0$ (by problem setting); which guarantees that chance-constraints will be automatically satisfied in the current context.

therefore, the energy cost for FAR provision is not considered here.

As given in [40], forecasted WEM prices would be used to calculate the self-scheduling offers for the VPP. Based on the price-taker model, as shown in Fig. 1, the VPP will resort to self-scheduling bidding strategy [19] for WEM participation to assist in the calculation of locational marginal prices (LMPs) or, simply, the prices. The retail price of electricity (such as TOU tariff) for consumers is typically predetermined [7]. These prices will be determined based on the regulator's recommendations to ensure the revenue sufficiency of the VPP. However, the calculation of such retail pricing is beyond the scope of this work. REGs, BSDs, and diesel generators (DGs) are paid for their declared operating costs. Profit-maximizer VPPs need to recover the cost of energy, PFR, and FAR provision. Some customers are allowed to participate in the demand response (DR) program, and the associated model is described in the next subsection. A quadratic cost function of dispatchable DGs is considered. Alternatively, with retail competition, both the loads and the DERs are expected to compete, and reserve requirements would have to be suitably bounded based on customer-submitted bids. But, the retail market could only operate in real-time, limiting the scope of associated research in the current context. Incentives related to the local reactive power provision are not considered in this work.

B. Customer Demand Response

Customers are expected to modify their electricity consumption based on the electricity price signal in the price-based DR programs. The relationship among electricity consumption $P_{q,t}^{DR}$ of the customer located at bus q, and the retail price π_t^{DR}, can be obtained from [41]. The electricity consumption can be calculated as follows:

$$P_{q,t}^{DR} = P_{q,t}^{L} \sum_{\forall y \in \mathcal{L}} \gamma_{q,y,t} \mathfrak{L}_y; \gamma_{q,y,t} \in \{0,1\}; \quad \forall q,t \tag{15}$$

$$\sum_{\forall y \in \mathcal{L}} \gamma_{q,y,t} = 1; \quad \forall q,t \tag{16}$$

where, $P_{q,t}^{L}$ is the forecasted load demand. $\gamma_{q,y,t}$ indicates the availability of a customer located at bus q, at time t, with demand response level, y. Also, $\mathfrak{L}_y$ represents various load levels. DR of the controllable loads can be given by $P_{q,t}^{DR}$. Two constraints, namely, non-increment of customers' total expenditure and non-decrement of customers' total daily consumption, have also been incorporated. Once the self-scheduling is carried out, the hierarchical autonomous controllers for each of the demand-responding customers would be provided with the advisory information for real-time operation.

C. Scheduling Strategies

The VPPs would participate to maximize their operational profit. Due to the associated lower probability of occurrence, the impact of permanent faults is not considered in this work but could be incorporated considering the reconfigurability of the network. The objective function of the chance-constrained joint-scheduling problem can be given as follows:

$$\max \quad -\mathfrak{C}^{WEM} - \mathfrak{C}^{DG} - \mathfrak{C}^{DiG} + \mathfrak{C}^{DR} - \mathfrak{C}^{B} \tag{17}$$

where,

$$\mathfrak{C}^{WEM} = \sum_{\forall t \in \mathcal{T}} k_t \pi_t^E P_{0,t}^G + \sum_{\forall t \in \mathcal{T}} \pi_t^{RS} S_{0,t} + \sum_{\forall t \in T} \pi_t^{RF} E_{0,t}^{BR} \tag{18}$$

$$\mathfrak{C}^{DG} = k_t \sum_{\forall t \in \mathcal{T}} \sum_{\forall q \in \mathcal{I}} \mathscr{F}(P_{q,t}^{DG} + S_{q,t}^{DG}) \tag{19}$$

$$\mathfrak{C}^{DiG} = k_t \sum_{\forall t \in \mathcal{T}} \sum_{\forall q \in \mathcal{I}} \mathrm{D}_q^{DiG} \left(P_{q,t}^{DiG} + E_{q,t}^{DiG}\right) \tag{20}$$

$$\mathfrak{C}^{B} = k_t \sum_{\forall t \in \mathcal{T}} \sum_{\forall q \in \mathcal{I}} \mathrm{D}_q^{B} \left(P_{q,t}^{B,-} + P_{q,t}^{B,+} + E_{q,t}^{B}\right) \tag{21}$$

$$\mathfrak{C}^{DR} = k_t \sum_{\forall t \in \mathcal{T}} \sum_{\forall q \in \mathcal{I}} P_{q,t}^{L} \pi_t^{DR} \sum_{\forall y \in \mathcal{L}} \gamma_{q,y,t} \mathfrak{L}_y \mathscr{P}_y^{DR} \tag{22}$$

$$\sum_{\forall y \in \mathcal{L}} \gamma_{q,y,t} = 1; \quad \forall q,t \tag{23}$$

$$P_{q,t}^{tot} = P_{q,t}^{DiG} + P_{q,t}^{DG} + P_{q,t}^{B,+} - P_{q,t}^{B,-} - P_{q,t}^{DR}; \ \forall q,t \tag{24}$$

$$E_{q,t}^{tot} = E_{q,t}^{DiG} + E_{q,t}^{DR} + E_{q,t}^{B}; \quad \forall q,t \tag{25}$$

$$P_{q,t}^{DiG} \geq 0; P_{q,t}^{DG} \geq 0; P_{q,t}^{B,+} \geq 0; P_{q,t}^{B,-} \geq 0; P_{q,t}^{DR} \geq 0; \ \forall q,t \tag{26}$$

$$E_{q,t}^{DiG} \geq 0; E_{q,t}^{DR} \geq 0; E_{q,t}^{B} \geq 0; \quad \forall q,t \tag{27}$$

subject to,

$$\Xi_t^+ + \frac{1}{1-\kappa} \sum_{\forall \xi \in \mathcal{N}} \mathbb{P}_{\xi,t} \beta_{\xi,t}^+ \leq 0; \quad \forall t \tag{28}$$

$$\sum_{\forall q \in \mathcal{I}} P_{q,t}^{tot} \mathrm{A}_{\xi,q} - \sum_{\forall q \in \mathcal{I}} E_{q,t}^{tot} \left(1 - \mathrm{A}_{\xi,q}\right) - E_{0,t}^{BR} - \Xi_t^+ - \beta_{\xi,t}^+ \leq 0; \quad \forall \xi,t \tag{29}$$

$$\beta_{\xi,t}^+ \geq 0; \quad \forall \xi,t \tag{30}$$

$$\Xi_t^- + \frac{1}{1-\kappa} \sum_{\forall \xi \in \mathcal{N}} \mathbb{P}_{\xi,t} \beta_{\xi,t}^- \leq 0; \quad \forall t \tag{31}$$

$$-\sum_{\forall q \in \mathcal{I}} P_{q,t}^{tot} \mathrm{A}_{\xi,q} - \sum_{\forall q \in \mathcal{I}} E_{q,t}^{tot} \left(1 - \mathrm{A}_{\xi,q}\right) - E_{0,t}^{BR} - \Xi_t^- - \beta_{\xi,t}^- \leq 0; \quad \forall \xi,t \tag{32}$$

$$\beta_{\xi,t}^- \geq 0; \quad \forall \xi,t \tag{33}$$

$$\sum_{\forall q \in \mathcal{I}} C_{q,l} P_{q,t}^{tot} = P_{l,t}^{flow}; \ -\sum_{\forall q \in \mathcal{I}} C_{q,l} Q_{q,t}^{DR} = Q_{l,t}^{flow}; \ \forall l,t \tag{34}$$

$$V_q^{min} \leq V_{q+1,t} = V_{q,t} - \frac{r_l P_{l,t}^{flow} + x_l Q_{l,t}^{flow}}{V_{0,t}} \leq V_q^{max}; \quad \forall q,t \tag{35}$$

$$\left(P_{l,t}^{flow}\right)^2 + \left(Q_{l,t}^{flow}\right)^2 \leq \mathcal{S}_l^2; \quad \forall l,t \tag{36}$$

$$\sum_{\forall q \in \mathcal{I}} S_{q,t}^{DG} + S_{0,t} \geq \mathrm{RUD}_t; \quad \forall t \tag{37}$$

$$P_{q,t}^{DG} + S_{q,t}^{DG} \leq P_q^{DG,max} \mathcal{J}_{q,t}; \quad \forall q,t \tag{38}$$

$$P_q^{DG,min}\mathcal{J}_{q,t} \le P_{q,t}^{DG} \le P_q^{DG,max}\mathcal{J}_{q,t}; \quad \forall q,t \tag{39}$$

$$P_q^{DG,min}\mathcal{J}_{q,t} \le P_{q,t}^{DG} - S_{q,t}^{DG}; \quad \forall q,t \tag{40}$$

$$-k_t\mathfrak{R}_{q,t+1}^{DG} + S_{q,t+1}^{DG} \le P_{q,t+1}^{DG} - P_{q,t}^{DG} \le k_t\mathfrak{R}_{q,t+1}^{DG} - S_{q,t+1}^{DG}; \quad \forall q,t \tag{41}$$

$$0 \le P_{q,t}^{DiG} \le P_{q,t}^{DiG,MPP}; \quad \forall q,t \tag{42}$$

$$0 \le P_{q,t}^{DiG} - E_{q,t}^{DiG}; P_{q,t}^{DiG} + E_{q,t}^{DiG} \le P_{q,t}^{DiG,MPP}; \quad \forall q,t \tag{43}$$

$$P_{q,t}^{DR} + E_{q,t}^{DR} = P_{q,t}^{L}\sum_{\forall y\in\mathcal{L}}\gamma_{q,y,t}\mathfrak{L}_y \le P_{q,t}^{L,max}; \quad \forall q,t \tag{44}$$

$$P_{q,t}^{L,min} \le P_{q,t}^{DR} - E_{q,t}^{DR}; \quad \forall q,t \tag{45}$$

$$\sum_{\forall t\in\mathcal{T}} P_{q,t}^{DR} \ge \sum_{\forall t\in\mathcal{T}} P_{q,t}^{L}; \quad \forall q \tag{46}$$

$$\sum_{\forall t\in\mathcal{T}} P_{q,t}^{L}\pi_t^{DR}\sum_{\forall y\in\mathcal{L}}\gamma_{q,y,t}\mathfrak{L}_y\mathscr{P}_y^{DR} \le \sum_{\forall t\in\mathcal{T}} P_{q,t}^{L}\pi_t^{DR}; \ \forall q \tag{47}$$

$$P_{q,t}^{L}\sum_{\forall y\in\mathcal{L}}\gamma_{q,y,t}\mathfrak{L}_y \le P_{q,t}^{L,max};$$

$$P_{q,t}^{L}\sum_{\forall y\in\mathcal{L}}\gamma_{q,y,t}\mathfrak{L}_y \ge P_{q,t}^{L,min}; \quad \forall q,t \tag{48}$$

$$Q_{q,t}^{DR} = \frac{\sqrt{1-\mathrm{pf}_q^2}}{\mathrm{pf}_q}P_{q,t}^{DR}; \quad \forall q,t \tag{49}$$

$$\mathbb{B}_{q,t+1} = \mathbb{B}_{q,t} + k_t\left(P_{q,t}^{B,+}\eta_{ch}z_{q,t} - P_{q,t}^{B,-}(1-z_{q,t})/\eta_{dch}\right);$$

$$\mathbb{B}_{q,0} = \mathbb{B}_q^{ini} = \mathbb{B}_{q,N}; \quad \forall q,t \tag{50}$$

$$-P_q^{B,max} \le -P_{q,t}^{B,-} - E_{q,t}^{B}; \quad \forall q,t \tag{51}$$

$$P_{q,t}^{B,+} + E_{q,t}^{B} \le P_q^{B,max}; \quad \forall q,t \tag{52}$$

$$\mathbb{B}_q^{min} \le \mathbb{B}_{q,t} \le \mathbb{B}_q^{max}; \quad \forall q,t \tag{53}$$

$$\mathbb{B}_q^{min} + \frac{E_{q,t}^{B}}{\eta_{dch}}\tau \le \mathbb{B}_{q,t} \le \mathbb{B}_q^{max} - \eta_{ch}E_{q,t}^{B}\tau; \quad \forall q,t \tag{54}$$

The objective function (17) aims to maximize the daily operational profit of the VPP from the day-ahead operational point of view. Revenues from DR tariffs given the retail prices, the operating cost of REGs, DGs, revenues from the DR program, and operational expenses of BSDs are given in (18)-(22).

REGs operate below their maximum power level for participation in both energy and FAR provisions. A well-discussed, linear operational cost model for both REGs and BSDs as shown in (20) and (21), are considered here. Consideration of absolute values in the BSD cost model ensures accounting for capacity depreciation (or throughput, as considered in [42]) during both charging and discharging. The cost functions include the opportunity cost for providing the reserve. All the loads are price responsive and assumed to be able to participate in the FAR provision (utilizing associated storage devices). The associated response level is identified by the binary variable $\gamma_{q,l,t}$. The revenue generated from the DR provision is given in (22).

The set of constraints associated with the CVaR problem need to be individually satisfied during all the operating intervals for the individual chance-constrained problem and are given in (28)-(30) and (31)-(33) (see [31]). The power flow equations are obtained by utilizing the method described in [43]. The branch flow equations are derived using (34), and node voltages can be calculated using (35). The node voltages should remain within the stipulated limits of 0.95 *pu* to 1.05 *pu*, subject to the substation remaining at a predefined $V_{0,t}$ *pu*. Equation (36) indicates the security constraints of a PDS, while (37) constrains the simplistic network PFR requirement to mitigate load and renewable uncertainties. Equations (39)-(40) depict active power and PFR provisions from DGs. The ramp-rate limit of DGs is presented in (41), which ensures the possible provision of the PFR requirement from DGs.

Constraints in (42) and (43) limit energy and FAR provision from the REGs. Equations (44) and (45) constrain the DR provision such that the customer power consumption remains within limits. Equation (46) ensures that the energy consumption of responsive loads remains bounded. Additionally, (47) ensures that the total revenue received from the DR is limited to the revenue generated without DR. Equation (48) indicates the convenience limit of loads. Equation (49) calculates the reactive power demand of the DR loads considering a constant load power factor. Equation (50) can be used to calculate the amount of charge stored within the battery. Power injection and extraction from BSD are also limited by converter capacity and are given in (51) and (52), respectively. Equation (53) imposes a capacity constraint on the operation of the BSDs. As discussed earlier in this section, considering that the FAR provisioning arrangement is required for the duration of τ, (54) limits the energy level of BSDs for FAR provision.

Some of the nonlinear equations above are suitably linearized, and therefore, the proposed scheduling problem is MILP in nature. Polynomial approximate of the flow limits (see, section 6.3.4 in [24]) of the devices has no impact in terms of the feasibility of the solution. The complexity is expected to rise considerably with detailed models, such as AC power flow equations, which have not been considered due to the limited scope of this work.

IV. Illustration

It is imminent from Section II that FAR requirements depend upon energy schedules. Local PFR requirements create additional constraints in the scheduling problem. This has motivated us to analyze the combined day-ahead energy, reserve joint schedule, and understand the rationale behind optimal choices the decision-maker suggests. It has also helped us understand the impact of the probabilistic nature of recloser operation in the proposed chance-constrained problem. The dataset used to study the impact of the chance-constraint on the energy schedule of the VPP is described next.

A modified[5] IEEE 33-bus radial test system, entirely managed by the VPP operator, is considered for analysis. Locations of reclosers, DGs, REGs, and BSDs in the network are depicted in Fig. 3. The scope of operation of the VPP is highlighted. Geographically dispersed multiple PDS can also be considered in this regard without loss of generality. Branch and load data of the standard benchmark IEEE 33-bus

[5]IEEE 33-bus PDS is modified to incorporate reclosers. Locations of fuses were not considered because of fuse-saving operation due to temporary faults. Sectionalizers are not considered here but can be suitably incorporated.

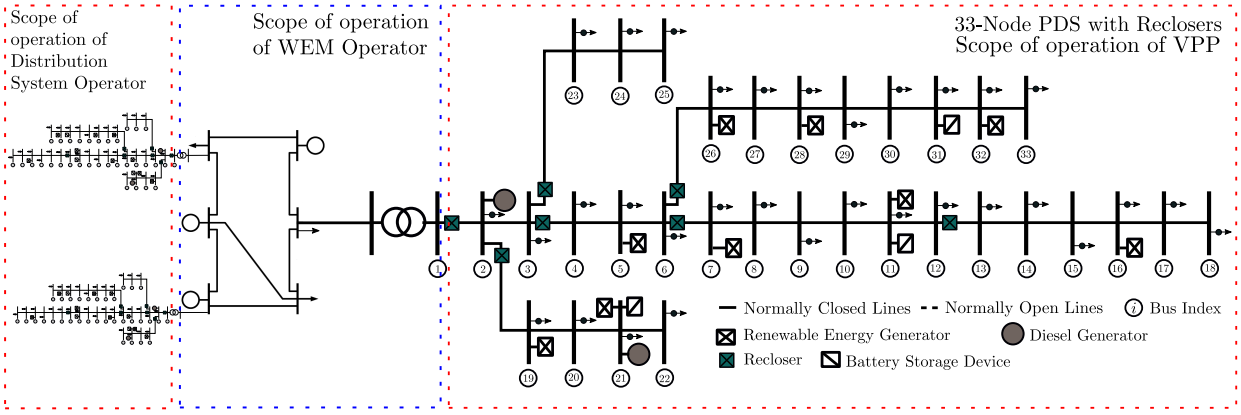

Figure 3: Modified multiple IEEE 33-bus radial distribution test system interfaced with IEEE 6-bus transmission system.

are obtained from [44]. Branches of the radial network are considered to be one km long, with the fault rate of 1.14×10^{-3} faults/hour-km on the scheduled day during all operating hours (the fault rate can vary during different operating intervals). The presented fault-rate is based on the typical fault rate obtained from [14] and the assumptions that most of the faults occur within a certain, high fault-rate period of the year [25]. The scheduled day is divided into 24 hourly intervals. From the day-ahead point of view, the occurrence of faults can be treated as random events.

Consequently, hourly event occurrence probabilities for the scheduled day (calculated using Remark 1) are given in Table I. For example, event one is triggered by the occurrence of faults in line segments 1-2 and 2-3 (in accordance with Definition 1). The majority of the faults would lead to the operation of multiple reclosers to prevent other DERs from feeding the fault; for example, during event one, reclosers connected between 1-2, 2-19, 3-4, and 3-23 would operate (probability would be = 1.14×10^{-3} faults/hour-km $\times$ 1 hour $\times$ 100% $\times$ 2 km $=$ 0.228%). Given that the network is operated radially, exactly one of the reclosers would carry the fault-current emanating from the substation and is identified as the immediate upstream recloser. In this work, the event[6] is specified by the operation of the immediate upstream recloser (assuming other reclosers would also operate) as given in Table I. Event 0 signifies the operation of none of the reclosers.

Table I: Probability of Events

Event	0	1	2	3	4	5	6	7
ξ	NOP	1-2	3-4	6-7	12-13	2-19	3-23	6-26
$\mathbb{P}_{\xi,t}$ (%)	96.35	0.23	0.34	0.68	0.68	0.46	0.34	0.91

The load profile is considered to vary throughout the day, and the load data available in [44] is considered to be corresponding to the peak-load profile. An interval-wise load profile is presented in Fig. 4a, and the reactive power demand is calculated by assuming that the peak load power factor remains constant. A line-flow limit of 5 MVA is considered for all the network lines as a part of the security constraint. As shown in Table II, ten different levels of load demand and associated prices for DR loads based on [45] are considered. The price-responsive loads can participate both in energy shifting and providing FAR.

Table II: Price-Based Demand Response Dataset

$\mathfrak{L}_y$	70	80	90	100	110	120	130	140	150	160
$\mathscr{P}_y^{DR}$	108	105	102	100	98	96	95	93	92	91

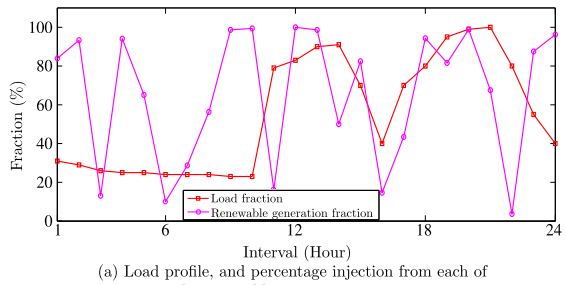

(a) Load profile, and percentage injection from each of the renewable energy generators.

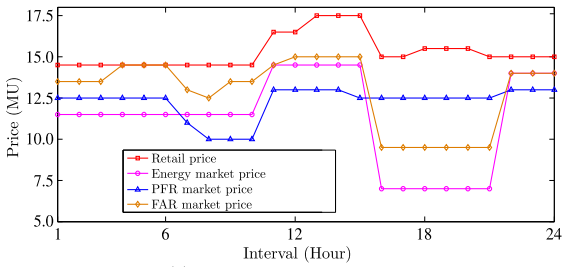

(b) Price data for the scheduled day.

Figure 4: Forecasted Dataset for the scheduled day.

The retail base price of electricity for customers, given in Fig. 4b, satisfies the pricing set by the regulator (market arrangements are briefly discussed in Section III-A). Ratings of DGs present within the network are provided in Table III. DGs have a finite ramp rate and hence are unable to

[6]In this work, we have considered that the network is not reconfigurable, which makes identification of the events straightforward. Due to the static nature of the problem, event types could be identified apriori, as discussed here. However, As discussed in Definition 1, events are identified by the occurrence of faults in the line between adjacent reclosers, the calculation of which would increase complexity of the overall problem formulation. Nevertheless, since the overall problem is being looked at from a day-ahead point of view, the network could be appropriately reconfigured for profit maximization; and reconfiguration-related constraints would be a part of overall problem formulation.

participate in FAR provision. The cost of DGs is given by $0.01\left(P_{q,t}^{DG}\right)^2+8.5P_{q,t}^{DG}$ MU/kW. Suppose that the cost function can be represented through a set of affine approximates, given by, $\mathrm{a}_{kk}P_{q,t}^{DG}+\mathrm{b}_{kk}$, then, given the underlying convexity of the cost function, the operational cost of the DG for a given power delivered, $P_{q,t}^{DG}$, can be given by,

$$\min \mathscr{A}$$
$$\mathscr{A} \geq \mathrm{a}_{kk}P_{q,t}^{DG}+\mathrm{b}_{kk}; \qquad \forall P_{q,t}^{DG}$$

Since, the aim is to minimize the operational cost of DGs, (19) can be simply represented by a set of linear inequalities given by, $\mathfrak{C}_{q,t}^{DG} \geq \mathrm{a}_{kk}\left(P_{q,t}^{DG}+S_{q,t}^{DG}\right)+\mathrm{b}_{kk}; \quad \forall kk$. Additionally, $\mathfrak{C}^{DG}$ in the objective function (17) can be represented by $\sum_{\forall t\in\mathcal{T}}\sum_{\forall q\in\mathcal{I}}\mathfrak{C}_{q,t}^{DG}$. The DG cost function is to be constituted of two piece-wise segments. Here, MU represents an arbitrary monetary unit.

Table III: Parameters for Scheduling

Resource	Parameters	Values
Diesel Generator	$P_{(\cdot)}^{DG,min/max}$	50 / 450 kW
REGs	$P_{(\cdot)}^{DG,max/min}$	100 / -100 kW
	$\mathrm{D}_{(\cdot)}^{DiG}$	8.10 MU/kW
BSDs	$P_{(\cdot)}^{\mathcal{B},max}$	400 kW
	$\mathrm{D}_{(\cdot)}^{\mathcal{B}}$	8.10 MU/kW
	$\mathbb{B}_{(\cdot)}^{ini/min/max}$	0.5 / 0.1 / 0.9 $\mathrm{Cap}_{(\cdot)}^{\mathcal{B}}$
	$\mathrm{Cap}_{(\cdot)}^{\mathcal{B}}$, τ	4000 kWh, 60 s
	η_{ch}, η_{dch}	0.95
Network	$V_{(\cdot)}^{max}, V_{(\cdot)}^{min}$	1.05 pu, 0.90 pu
	RUD_t	$\pm$10% of Load Demand
	κ	0.999

Various financial and operational parameters of REGs and BSDs, network operating limits, and confidence level of the chance-constrained problem are presented in Table III. All DGs, REGs, and BSDs are identical in terms of their capacities and ratings. Because BSDs provide FAR utilizing the stored energy, the FAR provision is considered to be limited to a maximum duration of 60 seconds (deadtime for fast-switching, during which FAR will be needed, is much less than this maximum duration). REGs are considered to be of 100 kWp, and the associated maximum power production level is based on the forecast depicted in Fig. 4a. These generators are designed to operate below the maximum power points, to supply both up and down FAR. As already discussed, energy and fast-acting and PFR can be procured from the WEM (briefly discussed in Section III-A), and the associated price profile is given in Fig. 4b.

A. Energy, FAR and PFR at Interplay

Given the local active power, PFR, and FAR provisions for the given dataset presented in Figs. 5 and 6, respectively, the procurement schedule of these resources from the WEM is shown in Fig. 7. Note that BSDs, REGs, and DR resources participate in FAR provision, while only DGs participate in PFR provision. Specific observations are discussed in the following paragraphs.

During intervals 1-10 h, both load demands and renewable generation are relatively low. Given the finite capacity and marginal costs, the local resources can satisfy local demand. Comparing the marginal costs of DGs, energy market price, and PFR price, it is profitable for the DGs to trade PFR (as seen in Fig. 7) into the WEM. DGs also charge up BSDs (as seen in Fig. 5) to exercise shifting opportunities later during the day. Lower renewable generation implies negligible contribution from REGs towards the FAR. Given that the marginal cost of FAR provision is lower than the retail rate, customers benefit from DR strategy to provide FAR. Since the FAR requires energy provision only for a short duration of time (before other reserves catch up), BSDs can provide FAR. Therefore, the VPP can satisfy the majority of energy and FAR demand locally and can sell excess PFR (as seen in Fig. 7).

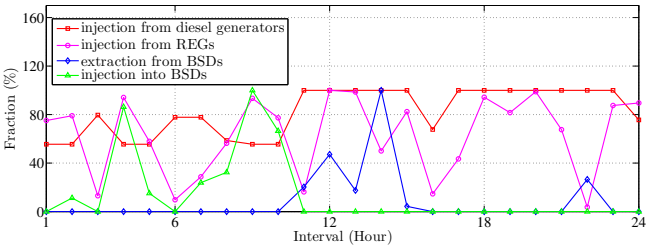

Figure 5: Active power generation schedule from local generators (DGs = 900.00 kW, REGs = 900.00 kW, BSDs Discharging = 618.83 kW, BSDs Charging = 441.31 kW corresponding to 100% fraction).

During intervals 11-15 h, loads become significantly higher (as seen in Fig. 4a), and it is expected that both PFR and FAR requirements would also grow significantly. Since the offering price of the PFR is lower than both retail and energy WEM prices (as seen in Fig. 4b), DGs do not provide the PFR (as seen in Fig. 5). High enough retail price and load demand induce BSDs to discharge (as seen in Fig. 5). Retail prices are equal to or higher than WEM FAR price, which implies that some customers would still provide FAR through DR. From (22), it can be seen that the customers are charged based on their energy consumption at the retail rate coupled with DR rate, and a fraction of their consumption would be used to satisfy the FAR requirement. Additionally, (47)-(48) states that, in this process, total energy consumption does not decrease, and customer benefit would still be higher if they pay the retail price alone. While the net energy requirement can be considerably low, participation in FAR provision would reduce power injection from associated inverters in energy provision (see (51)-(52)). The comparatively high retail price and insufficient local resources to capture local load demand imply that BSDs and REGs won't be called in to provide FAR.

During intervals 16-21 h, since the WEM resources' marginal energy prices are considerably lower than the unit price of local resources, one can expect non-participation of local resources in the energy provision. However, non-provision of the local resources would induce substantial load-generation imbalance, resulting in a higher FAR requirement with higher marginal cost, inducing participation of both REGs and DGs to satisfy the local energy demand. During

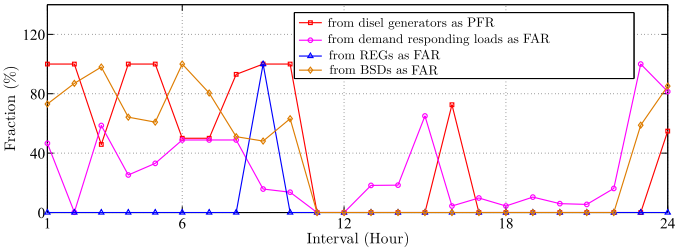

Figure 6: PFR and FAR provision from local generators (DGs = 400.00 kW, DR = 143.34 kW, REGs = 47.24 kW, BSDs = 334.21 kW corresponding to 100% fraction).

intervals 22-24 h, marginal prices of local resources again become comparatively low. Therefore, one can observe the participation of BSDs, WTGs, and DGs in meeting the load demand at 22 h (as seen in Fig. 5). During the successive intervals, the load demand reduces and participation of REGs increases. Additionally, local provision of both PFR and FAR become cost-effective once again (as seen in Figs. 7 and 8).

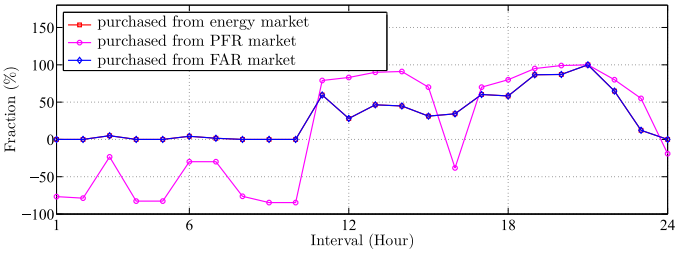

Figure 7: Participation into the electricity market (energy market = 2.49 MW, PFR = 371.50 kW, FAR = 2.49 MW corresponding to 100% fraction).

B. Lost FAR

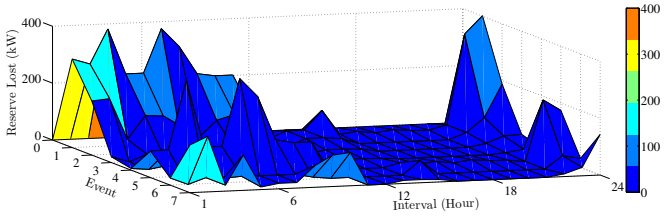

Figure 8: Loss of available reserve throughout the day.

Given various marginal prices, loads, and renewable generation forecasts at interplay, local resources provide FAR only during certain intervals as discussed earlier. Depending upon the locations of reclosers (defined in Table I) defining various events, interval-wise lost FAR is shown in Fig. 8. It is to be noted that despite lower WEM prices, during certain instances, local resources will be called in to participate, in order to reduce FAR requirements. The optimal solution implies that the VPP will meet FAR requirements with a 99.9% confidence level despite these reserve losses. It can be expected that the VPP may be able to reduce FAR imports with increasing penetration of local resources.

C. Parametric Analysis for Different Confidence Levels and Contrasting the Solution with Worst-Case Optimal Solution

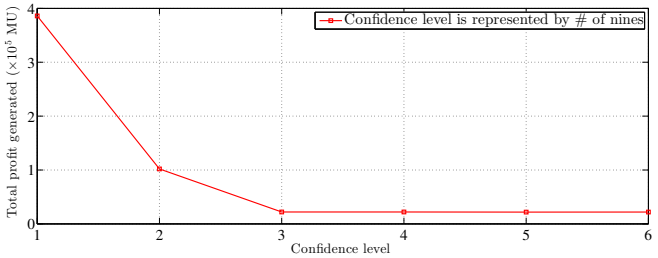

Figure 9: Total profit generated by the VPP with increasing confidence level.

The probability of the occurrence of recloser 1-2 operation is the lowest at 0.23% (event 1, in Table I). Therefore, a confidence level of more than (=100.00-0.23 %) 99.77% would result in an asymptotic behavior of the total profit generation characteristics of the VPP. Looking at both Figs. 8, 9, purchase from WEM is equal to FAR procurement, implying, despite FAR losses, VPP has procured sufficient reserve to meet all possible imbalance conditions. This characteristic is shown in Fig. 9. However, the confidence level will be dictated by the WEM operator to ensure that the local events remain contained.

For the worst-case joint-scheduling problem, we have limited ourselves to Remark 1, which assumes the occurrence of more than one event within a given interval will be approximately zero. The associated constraints within the problem would be:

$$P^{Imb}_{\xi,t} - E^{Imb}_{\xi,t} \leq 0; \quad \forall \xi, t$$
$$-P^{Imb}_{\xi,t} - E^{Imb}_{\xi,t} \leq 0; \quad \forall \xi, t$$

The solution to the revised OPF exists, and as expected from the discussion above, the solution of the worst-case scheduling problem coincides with the solution obtained with the confidence level of 99.77% (not discussed in detail for brevity).

D. Impact of Limited FAR on the System Performance

As given in Table III, the considered confidence level chosen in this work is 99.90%, which is more than the one required for asymptotic convergence. Therefore, as shown in Fig. 9, the worst-case FAR provision will be always satisfied. Therefore, a confidence level of 99% is considered in this subsection for analysis, and the participation in the energy and FAR market is shown in Fig. 10. A comparative analysis of Figs. 7 and 10, shows a change in energy and FAR procurement from the WEM. A relaxed confidence level indicates more energy is being procured from local DERs, at the expense of higher chances of insufficient FAR procurement.

The problem of insufficient FAR procurement has been demonstrated using a sample system discussed in [12], with inertial constant (H) of 10 s, system base (S_{base}) of 100 MW, damping ratio (D) of 0.3 pu-MW/Hz, system frequency (f_0) of 60 Hz, and regulation factor of 0.3 Hz/pu-MW. In a low inertia

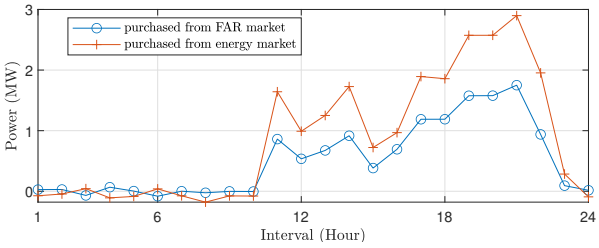

Figure 10: Participation into the electricity market with 99% confidence level.

system, frequency measurement will be inherently delayed, and we consider a delay (T_d) of 40 ms. We assume that the reserve available from the BPS is limited to procured level for this set of experiments. We also consider a deadtime of 150 ms for the recloser operation. Two cases are considered with the occurrence of event 1 during interval 21 at (i) 99.9% confidence and (ii) 99.0% confidence.

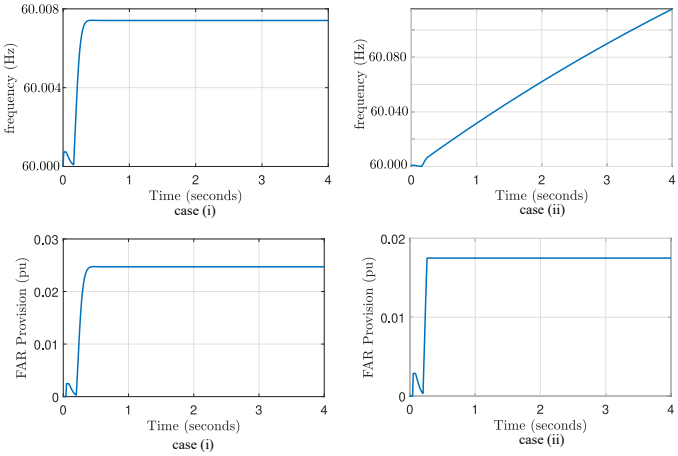

Figure 11: Comparative analysis of system performance with limited FAR.

The impact of the limited available reserve is shown using Fig. 11. Observed frequency response can be justified by the delayed reserve provision being comparatively small enough to allowable delay. Following the occurrence of event 1, BPS would have excess energy, therefore, both system frequency and FAR requirements are positive. Still, due to available low enough inertial reserve, the system encounters frequency excursion, which may result in triggering frequency relays within the BPS. Notably, in the current context, it is imminent that the FAR provision would be significantly more than the one considered for the simulation. However, as discussed earlier, if the BPS observes the occurrence of multiple faults, it may not have enough resources to cater to the events that are traditionally invisible, which makes this analysis justifiable.

E. Scalability of the Proposed Formulation

A moderately sized 98-node radial test system constituting of three identical 33-node feeders connected at the sub-station node, with similar locations of reclosers, DGs, DERs, and loads as discussed in one of our earlier research has been considered here to understand the scalability of the MIP problem. While the computation time with the IEEE 33-node system with a confidence level of 90% is $\approx$ 19s, the computation time with 98-bus system scales up to $\approx$ 78s. The complexity of the problem increases with increasing confidence level and therefore, with 33-node system with confidence levels 99% and 99.9% the computation time becomes $\approx$ 40s, and $\approx$ 87s, respectively. Please note that all these calculations were carried out in an Intel core-i7 platform with 16 GB RAM. As indicated earlier, complexity does not increase beyond 99.77%, and it is reflected in terms of the computation time. However, it is notable that the problem at hand is MIP, polynomial time convergence may not be guaranteed.

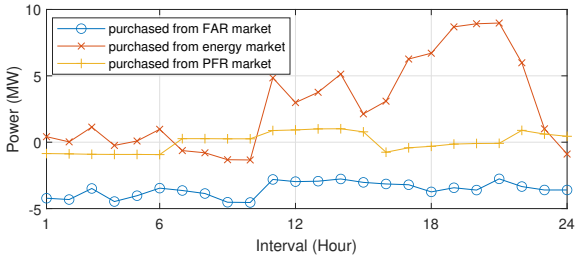

Figure 12: Participation into the electricity market with 90% confidence level with 98-node system.

Detailed analysis of individual resource response with a large test-system can be difficult, which is the primary reason behind choosing the said IEEE 33-node system. We have shown the performance of the proposed formulation with 98-node system in Fig. 12, where it can be seen that, if compared with the results of 33-node system, the WEM participation is scalable across all the test feeders. It can also be seen that with low enough confidence levels the VPP is able to sell FAR. However, it is to be notable that such a FAR provision into the BPS would also suffer from reserve provision confidence level of 90%, and the BPS operator would be aware of such non-provision.

V. Conclusions

This work has discussed the fast-acting reserve (FAR) requirements induced by stochastic fast-switching requirements in a futuristic low-inertia power system, considering temporary faults as a use-case. The power distribution system (PDS) is being operated as a virtual power plant (VPP). In this regard, the chance-constraints dictating FAR requirements are modeled as conditional value at risk (CVaR), considering both the FAR providing generators' unavailability and load-generation imbalance as a Poisson process. Individual chance-constraints have been utilized here for modeling simplicity. Here the VPP operator is expected to acquire sufficient FAR to cater to these events for a given confidence level. The allocation problem is modeled as a joint-schedule. The VPP operator is expected to procure resources for energy, and PFR and FAR provision from local resources or the wholesale market.

The proposed joint-scheduling problem is analyzed through a modified IEEE 33 bus radial PDS, while its scalability is verified using a 98-node test system. It has been shown that the increased FAR requirement to combat local power imbalance would influence the energy schedule; and, all three schedules are interlinked. The scheduling strategy and operating profit are reliant on the confidence level of the chance-constraint, and the increasing confidence level is shown to reduce the overall profit. The solution of the chance-constrained problem asymptotically converges to the worst-case solution with an increasing confidence level. CVaR is shown to be convex in the given case with no impact on the solution due to resulting simplification. Higher operational profit with a lower confidence level prevails because of the ability of the VPP to sell the FAR into the wholesale energy market (WEM). The impact of limited available reserves on system dynamic response has been demonstrated. Impacts of multiple faults including permanent faults, especially during extreme weather events, will be the subject of future work.

APPENDIX
DISCUSSIONS RELATED TO CHANCE-CONSTRAINTS

Suppose P_{ξ}^{Imb} and $-P_{\xi}^{Imb}$ are the excess load lost and excess generation lost, respectively. Also, E_{ξ}^{Imb} is the reserve requirement to cater to both of these lost load and generation requirements. With κ being the confidence level, the chance-constraints become:

$$\mathbb{P}\left(\sum_{\forall \xi \in \mathcal{N}} \left(-E_{\xi}^{Imb} + P_{\xi}^{Imb}\right) \mathbb{1}_{\mathcal{N}}(\xi) \leq 0\right) \geq \kappa$$

$$\mathbb{P}\left(\sum_{\forall \xi \in \mathcal{N}} \left(-E_{\xi}^{Imb} - P_{\xi}^{Imb}\right) \mathbb{1}_{\mathcal{N}}(\xi) \leq 0\right) \geq \kappa$$

Here, E_{ξ}^{Imb} is a non-negative real number. Therefore, $E_{\xi}^{Imb} - P_{\xi}^{Imb}$ and $E_{\xi}^{Imb} + P_{\xi}^{Imb}$ would have opposite signs, if, $P_{\xi}^{Imb} > E_{\xi}^{Imb} > 0$ or $P_{\xi}^{Imb} < -E_{\xi}^{Imb} < 0$, implying, either of the chance-constraints can be violated for a given ξ. Therefore, either of load and generation insufficiency related constraints would contribute to violation of each chance-constraints. Associated VaR constraints corresponding to the chance-constraints can be written as [31]:

$$\mathbb{P}\left(\sum_{\forall \xi \in \mathcal{N}} \left(-E_{\xi}^{Imb} + P_{\xi}^{Imb}\right) \mathbb{1}_{\mathcal{N}}(\xi) \leq 0\right) \geq \kappa$$

$$\Leftrightarrow \text{VaR}_{\kappa}\left(\sum_{\forall \xi \in \mathcal{N}} \left(P_{\xi}^{Imb} - E_{\xi}^{Imb}\right) \mathbb{1}_{\mathcal{N}}(\xi)\right) \leq 0$$

$$\mathbb{P}\left(\sum_{\forall \xi \in \mathcal{N}} \left(-E_{\xi}^{Imb} - P_{\xi}^{Imb}\right) \mathbb{1}_{\mathcal{N}}(\xi) \leq 0\right) \geq \kappa$$

$$\Leftrightarrow \text{VaR}_{\kappa}\left(\sum_{\forall \xi \in \mathcal{N}} \left(-P_{\xi}^{Imb} - E_{\xi}^{Imb}\right) \mathbb{1}_{\mathcal{N}}(\xi)\right) \leq 0$$

Given the non-convexity of VaR measure, we use CVaR measure given as:

$$\text{CVaR}_{\kappa}\left(\sum_{\forall \xi \in \mathcal{N}} \left(P_{\xi}^{Imb} - E_{\xi}^{Imb}\right) \mathbb{1}_{\mathcal{N}}(\xi)\right) \leq 0$$

$$\text{CVaR}_{\kappa}\left(\sum_{\forall \xi \in \mathcal{N}} \left(-P_{\xi}^{Imb} - E_{\xi}^{Imb}\right) \mathbb{1}_{\mathcal{N}}(\xi)\right) \leq 0$$

REFERENCES

[1] D. Pudjianto, C. Ramsay, and G. Strbac, "Virtual power plant and system integration of distributed energy resources," *IET Renew. Power Gen.*, vol. 1, no. 1, pp. 10–16, Mar. 2007.

[2] N. Naval and J. M. Yusta, "Virtual power plant models and electricity markets - a review," *Renewable and Sustainable Energy Reviews*, vol. 149, p. 111393, 2021.

[3] J. F. Venegas-Zarama, J. I. Muñoz-Hernandez, L. Baringo, P. Diaz-Cachinero, and I. De Domingo-Mondejar, "A Review of the Evolution and Main Roles of Virtual Power Plants as Key Stakeholders in Power Systems," *IEEE Access*, vol. 10, pp. 47 937–47 964, 2022.

[4] FERC, "FERC Order No. 2222: Fact Sheet," 2020.

[5] "Aggregate Distributed Energy Resource (ADER) ERCOT Pilot Project," 2022, public Utility Commission of Texas. [Online]. Available: https://interchange.puc.texas.gov/Documents/53911_18_1241809.PDF

[6] "Virtual Power Plant in South Australia," 2022, australian Renewable Energy Agency. [Online]. Available: https://arena.gov.au/assets/2021/05/advanced-vpp-grid-integration-final-report.pdf

[7] M. Badtke-Berkow, M. Centore, K. Mohlin, and B. Spiller, "A primer on time-variant electricity pricing," *Environmental Defense Fund*, 2015.

[8] H. Thiesen, C. Jauch, and A. Gloe, "Design of a system substituting today's inherent inertia in the european continental synchronous area," *Energies*, vol. 9, no. 8, Jul. 2016.

[9] P. Tielens and D. V. Hertem, "The relevance of inertia in power systems," *Renew. Sust. Energ. Rev.*, vol. 55, pp. 999 – 1009, Mar. 2016.

[10] A. Arana *et al.*, "Fast frequency response concepts and bulk power system reliability needs," in *NERC Inverter-Based Resource Performance Task Force (IRPTF)*, 2020.

[11] N. Miller, D. Lew, and R. Piwko, "Technology Capabilities for Fast Frequency Response," GE Energy Consulting, Tech. Rep., Mar. 2017.

[12] S. Majumder, A. P. Agalgaonkar, S. A. Khaparde, S. Perera, S. V. Kulkarni, and P. P. Ciufo, "Allowable Delay Heuristic in Provision of Primary Frequency Reserve in the Future Power System," *IEEE Trans. Power Syst.*, pp. 1–1, 2019.

[13] J. H. Eto, J. Undrill, C. Roberts, P. Mackin, and J. Ellis, "Frequency control requirements for reliable interconnection frequency response," 2018. [Online]. Available: https://eta-publications.lbl.gov/sites/default/files/frequency_control_requirements_lbnl-2001103.pdf

[14] T. A. Short, *Electric power distribution handbook*. CRC press, 2014.

[15] S. M. Brahma and A. A. Girgis, "Development of adaptive protection scheme for distribution systems with high penetration of distributed generation," *IEEE Trans. Power Del.*, vol. 19, no. 1, pp. 56–63, Jan. 2004.

[16] C. A. McCarthy and M. J. Meisinger, "Intelligent fuse-saving," in *11th IET International Conference on Developments in Power Systems Protection (DPSP)*, Apr. 2012, pp. 1–5.

[17] R. Nylen, "Auto-reclosing," *ASEA J.*, vol. 6, pp. 127–132, 1979.

[18] G. Antonova, M. Nardi, A. Scott, and M. Pesin, "Distributed generation and its impact on power grids and microgrids protection," in *2012 65th Annual Conference for Protective Relay Engineers*, 2012, pp. 152–161.

[19] California ISO, "Day-Ahead Market Enhancements," Tech. Rep., 2020, http://www.caiso.com/InitiativeDocuments/RevisedStrawProposal-Day-AheadMarketEnhancements.pdf.

[20] F. S. Gazijahani and J. Salehi, "Igdt-based complementarity approach for dealing with strategic decision making of price-maker vpp considering demand flexibility," *IEEE Transactions on Industrial Informatics*, vol. 16, no. 4, pp. 2212–2220, 2020.

[21] Y. Zhang, F. Liu, Z. Wang, Y. Su, W. Wang, and S. Feng, "Robust scheduling of virtual power plant under exogenous and endogenous uncertainties," *IEEE Transactions on Power Systems*, pp. 1–1, 2021.

[22] M. Yazdaninejad, N. Amjady, and S. Dehghan, "Vpp self-scheduling strategy using multi-horizon igdt, enhanced normalized normal constraint, and bi-directional decision-making approach," *IEEE Transactions on Smart Grid*, vol. 11, no. 4, pp. 3632–3645, 2020.

[23] A. Jamali, J. Aghaei, M. Esmaili, A. Nikoobakht, T. Niknam, M. Shafiekhah, and J. P. S. Catalão, "Self-scheduling approach to coordinating wind power producers with energy storage and demand response," *IEEE Transactions on Sustainable Energy*, vol. 11, no. 3, pp. 1210–1219, 2020.

[24] S. Majumder, "Techno-Economic Analysis of Electricity Networks with Renewable Energy Sources and Storage Devices," Ph.D. dissertation, School of Electrical, Computer and Telecommunications Engineering, University of Wollongong, 2019, https://ro.uow.edu.au/theses1/709.

[25] M. H. Bollen, *Understanding Power Quality Problems: Voltage Sags and Interruptions*. Wiley, 2000.

[26] S. Sheng, D. Xianzhong, and W. L. Chan, "Probability distribution of fault in distribution system," *IEEE Transactions on Power Systems*, vol. 23, no. 3, pp. 1521–1522, 2008.

[27] C.-H. Park, G. Jang, and R. J. Thomas, "The influence of generator scheduling and time-varying fault rates on voltage sag prediction," *IEEE Trans. Power Deliv.*, vol. 23, no. 2, pp. 1243–1250, 2008.

[28] W. Thompson, *Point process models with applications to safety and reliability*. Springer Science & Business Media, 2012.

[29] Q. Chen, *The probability, identification, and prevention of rare events in power systems*. Iowa State University, 2004.

[30] A. Nemirovski and A. Shapiro, "Convex approximations of chance constrained programs," *SIAM Journal on Optimization*, vol. 17, no. 4, pp. 969–996, 2007.

[31] S. Sarykalin, G. Serraino, and S. Uryasev, "Value-at-risk vs. conditional value-at-risk in risk management and optimization," in *State-of-the-art decision-making tools in the information-intensive age*. Informs, 2008, pp. 270–294.

[32] R. Huisman, C. Huurman, and R. Mahieu, "Hourly electricity prices in day-ahead markets," *Energy Econ.*, vol. 29, no. 2, pp. 240 – 248, 2007.

[33] R. Kiesel and F. Paraschiv, "Econometric analysis of 15-minute intraday electricity prices," *Energy Econ.*, vol. 64, pp. 77 – 90, 2017.

[34] M. Caramanis and J. M. Foster, "Management of electric vehicle charging to mitigate renewable generation intermittency and distribution network congestion," in *Proceedings of the 48h IEEE Conference on Decision and Control (CDC) held jointly with 2009 28th Chinese Control Conference*, Dec. 2009, pp. 4717–4722.

[35] L. Roald and G. Andersson, "Chance-constrained AC optimal power flow: Reformulations and efficient algorithms," *IEEE Transactions on Power Systems*, vol. 33, no. 3, pp. 2906–2918, 2017.

[36] K. Baker and A. Bernstein, "Joint chance constraints in AC optimal power flow: Improving bounds through learning," *IEEE Transactions on Smart Grid*, vol. 10, no. 6, pp. 6376–6385, 2019.

[37] R. T. Rockafellar and S. Uryasev, "Optimization of Conditional Value-at-Risk," *J. Risk*, vol. 2, pp. 21–41, Apr. 2000.

[38] ——, "Conditional value-at-risk for general loss distributions," *Journal of banking & finance*, vol. 26, no. 7, pp. 1443–1471, 2002.

[39] S. Majumder and A. K. Srivastava, "Resilience-Driven Integration of Distributed Energy Resource (DER): Coordinating DER Services for Value," *IEEE SG eBulletin*, Sept. 2022.

[40] E. Mashhour and S. M. Moghaddas-Tafreshi, "Bidding strategy of virtual power plant for participating in energy and spinning reserve markets – part i: Problem formulation," *IEEE Trans. Power Syst.*, vol. 26, no. 2, pp. 949–956, May 2011.

[41] C. Zhang, Y. Xu, Z. Y. Dong, and K. P. Wong, "Robust coordination of distributed generation and price-based demand response in microgrids," *IEEE Trans. Smart Grid*, vol. 9, no. 5, pp. 4236–4247, Sept. 2018.

[42] S. Majumder, S. A. Khaparde, A. P. Agalgaonkar, P. Ciufo, S. Perera, and S. V. Kulkarni, "DFT-Based Sizing of Battery Storage Devices to Determine Day-Ahead Minimum Variability Injection Dispatch With Renewable Energy Resources," *IEEE Trans. Smart Grid*, vol. 10, no. 1, pp. 626–638, Jan. 2019.

[43] H. Yeh, D. F. Gayme, and S. H. Low, "Adaptive VAR Control for Distribution Circuits With Photovoltaic Generators," *IEEE Trans. Power Syst.*, vol. 27, no. 3, pp. 1656–1663, Aug. 2012.

[44] M. E. Baran and F. F. Wu, "Network reconfiguration in distribution systems for loss reduction and load balancing," *IEEE Trans. Power Del.*, vol. 4, no. 2, pp. 1401–1407, Apr. 1989.

[45] A. Khodaei, M. Shahidehpour, and S. Bahramirad, "SCUC with hourly demand response considering intertemporal load characteristics," *IEEE Trans. Smart Grid*, vol. 2, no. 3, pp. 564–571, Sept. 2011.